Rock Coating and Weathering-Rind Development at the Edge of Retreating Glaciers: An Initial Study

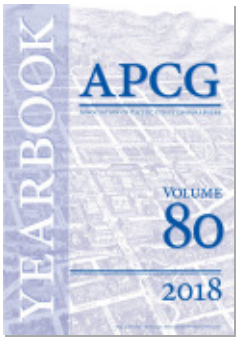

Ronald I. Dorn, Ara Jeong

Yearbook of the Association of Pacific Coast Geographers, Volume 80, 2018, pp. 66-96 (Article)

Published by University of Hawai'i Press
DOI: https://doi.org/10.1353/pcg.2018.0004

Rock Coating and Weathering-Rind Development at the Edge of Retreating Glaciers: An Initial Study

Ronald I. Dorn and Ara Jeong
Arizona State University

ABSTRACT

Six different electron microscope techniques imaged and analyzed boulder and bedrock surfaces with glacially polished textures collected from the margins of the Athabasca Glacier in Canada, Bunger Oasis of Antarctica, Franz Josef Glacier in New Zealand, a Greenland outlet glacier, the Ngozumpa Glacier in Nepal, and the Middle Palisade Glacier in California. The purpose of this pilot investigation involves developing a better understanding of both rock decay and rock coating development at the edge of retreating glaciers. Our hope is that others in the Association of Pacific Coast Geographers will test some of the findings of this research in their study areas. In research on rock decay, five different samples from the six contexts revealed the presence of weathering rinds with varying degrees of porosity ranging from 0.3 to 7.1 percent. An often-made assumption, inconsistent with these data, is that recently exposed glaciated rocks exist in a fresh or unaltered state and that progressive decay can be monitored by measurement of weathering-rind thicknesses or Schmidt Hammer measurements from this "initial state." The observed variability in weathering-rind porosity thus creates an additional uncertainty factor that could be incorporated into future studies of rock decay over time. Several different types of rock coatings occurred on the studied surfaces, including a newly recognized type of Mg-rich coating, iron films, rock varnish, fungal mats, and silica glaze—where silica glaze was the most commonly observed rock coating. The remobilized constituents of silica glaze, rock varnish, and iron also migrate into the underlying weathering rind to produce case hardening. Studies of rock varnish chemistry revealed evidence of twentieth- and twenty-first-century anthropogenic lead contamination in the upper micron of varnishes at the Greenland and Middle Palisade Glacier sites.

Keywords*: Anthropocene; dating method; glacial polish; lead pollution; paraglacial*

Introduction

The study of climate change and its impact on glacial fluctuations sometimes involves the measurement of rock decay, collecting field-based data on the state of rock decay on boulders in glacial moraines. Scholars in the Pacific Coast region have studied glacial moraines for just such a purpose for decades (e.g., Kesseli 1941; Whelan and Bach 2017). The purpose rests in trying to correlate deposits in different glacial valleys or continental ice lobes. Those studying rock decay, specifically the collection of field-based data as an indicator of time, necessarily make an assumption regarding recently deglaciated environments—that newly exposed rock surfaces exist in a "fresh" or unaltered condition.

An assumed lack of rock decay at "time zero" allows a starting point for such metrics as: (a) weathering-rind thickness (Burke and Birkeland 1979; Chinn 1981; Colman and Pierce 1981; Colman and Pierce 1986; Burbank and Cheng 1991; Ricker et al. 1993; Dabski and Tittenbrun 2013; Mills et al. 2017); (b) Schmidt hammer testing (McCarroll 1989; McCarroll 1994; Guglielmin et al. 2012; Dabski and Tittenbrun 2013; Kłapyta 2013; Foulkes and Harrison 2014; Reznichenko et al. 2016; Wilson et al. 2016; Zasadni and Kłapyta 2016); as well as (c) using weathering rinds as an indicator of past climates (Mahaney and Schwartz 2016) or preserving evidence of impact events (Mahaney and Keiser 2013).

Abundant research, however, reveals that solutes in glacial meltwater contain the products of rock-surface alteration prior to subaerial exposure at the edge of retreating glaciers (Fairchild et al. 1999). Chemical decay of rocks and minerals underneath glaciers results in highly variable abundances of ion concentrations of Ca^{2+}, Mg^{2+}, Na^{+}, K^{+} ,HCO_3^{-} , Cl^{-}, and SO_4^{2-} (Brown 2002). Subglacial processes include biotite decay (Anders et al. 2003), coupled oxidation of sulfide minerals and carbonate dissolution (Anderson et al. 2000), and silicate mineral dissolution (Graly et al. 2014). Subglacial decay under the Greenland ice sheet supplies substantial amounts of iron to the ocean (Bhatia et al. 2013), and solutes derived from glaciers impact global biogeochemical cycles (Wadham et al. 2013).

Bacteria and other microorganisms also play a substantial role in subglacial mineral decay (Skidmore et al. 2005, Graly et al. 2014), since bacteria provide an important source of protons (Sharp et al. 1999). Oxidation of iron in pyrite (Mitchell et al. 2013) provides energy for chemolithotrophic bacteria (Boyd et al. 2014). Subglacial bacteria studied at Svalbard are chemoheterotrophs that obtain energy by either organic or inorganic sources

and thus retain the ability to react quickly to more-favorable conditions (Kaštovská et al. 2007). Microorganisms appear to be more important beneath small valley glaciers (Wadham et al. 2010). In contrast, longer meltwater residence times underneath ice sheets enhance silicate dissolution due to abiotic processes (Wadham et al. 2010) that are magnified by the ability of glaciers to generate an abundance of fine-grained rock flour that increases the surface area exposed to chemical reactions (Anderson 2007).

The assumption of unaltered rock surfaces at the retreating margins of glaciers and observed high solute loads in glacial meltwater might or might not be incompatible. The rapid movement of water over small particles of glacial flour could potentially be responsible for observed dissolution rates in glaciated areas typically near or higher than continental averages (Tranter 2003).

Thus, this pilot study takes a different approach to evaluating the assumption of fresh rock at the margins of retreating glaciers. Rather than examining meltwater, *in situ* electron microscope examination of random samples of rock surfaces provides a different perspective on the state of rock decay for samples collected from the retreating margins of the Athabasca Glacier in Canada, Bunger Oasis of Antarctica, Franz Josef Glacier in New Zealand, a Greenland outlet glacier, the Ngozumpa Glacier in Nepal, and the Middle Palisade Glacier in California.

The first research problem posed in this study is whether *in situ* electron microscopy reveals evidence of rock surface alteration at the margins of retreating glaciers. The idea is to avoid samples that may have been exposed for decades, but only examine samples that have glacially polished textures collected at the glacier margin.

The second research problem deals with the nature of rock coatings on recently exposed rocks at glacier margins. Rock coating samples offer an opportunity to explore whether twentieth- and twenty-first-century anthropogenic lead might be contaminating recently exposed glacier margins, since the iron and manganese hydroxides in rock coatings record the deposition of anthropogenic lead (Dorn 1998; Spilde et al. 2013).

Study Sites and Sample Selection

The six glacier margins studied here contain different glacial and geological contexts (Table 1) that include ice sheet and alpine glacier margins and different rock types. Figure 1 exemplifies a field site—at the margin of a medial moraine of a Greenland outlet glacier. In each study site context,

five different samples with surface areas of about 10 cm^2 were selected from boulders or bedrock with glacially polished textures.

Table 1.—Sites where rock surfaces with a surface texture of glacial polish were collected in contact with the retreating margins of glacial ice.

Glacier	Coordinates	Rock Type	Surface
Athabasca Glacier, Canada	52.2085, -117.2343	limestone*	bedrock
Bunger Hills, Antarctica	-66.1957, 100.6689	quartz monzonite	boulder
Franz Josef Gl., New Zealand	-43.4489, 170.1743	schist	boulder
Greenland outlet glacier	- 63.5540, -50.5853	gneiss	boulder
Ngozumpa Glacier, Nepal	28.0069, 86.6898	gneiss	boulder
Middle Palisade Glacier, USA	37.0772, -118.4722	granodiorite	bedrock

*samples included zones with silicified nodules

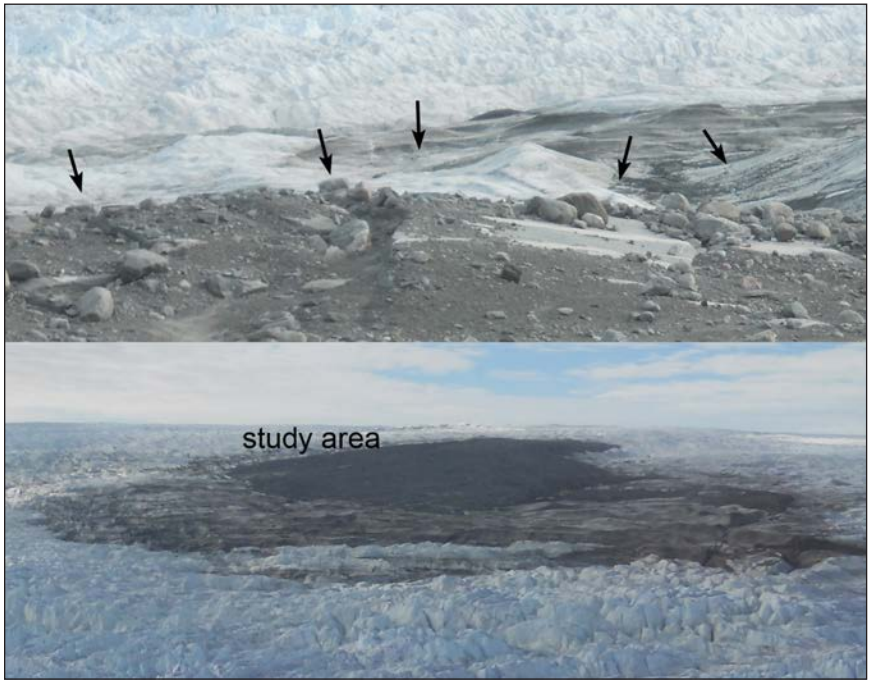

Figure 1.—Greenland outlet glacier study site on a medial moraine, identifying the first five boulders seen with a distinctive glacial polish texture in a random walk of the glacier margin.

The selection of the particular surfaces necessarily involved a random sampling strategy. Random sampling minimizes bias in selecting rock surfaces for subsequent analyses. For till boulders at the margins of ice, a walk was started at a randomly selected spot. The first five boulders with clear evidence of a glacially polished texture were sampled at their highest point above the ground. For glacially polished bedrock in contact with glacier ice, a coin was tossed. After bouncing and rolling, the location where the coin came to a stop was sampled with a rock hammer and chisel. The only exception to this sample selection process was the Bunger Hills, where R. Gerson (Hebrew University) generously supplied multiple samples from different boulders. Five of these samples with glacially polished textures were then selected randomly using dice.

Methods

Secondary electron (SE) microscopy, back-scattered electron (BSE) microscopy, high resolution transmission electron microscopy (HRTEM), energy dispersive spectroscopy (EDS), and wavelength dispersive spectroscopy (WDS) analyzed the samples (Reed 2005; Humphreys et al. 2014) collected from six margins of retreating glaciers (Table 1).

Millimeter-diameter chips of the samples were examined with SE, BSE, and EDS to develop a better understanding of rock decay and rock coatings. Where EDS detected the presence of lead, WDS of a JEOL superprobe electron microanalyzer quantified lead abundance under operating conditions of 20 nA, a take-off angle of 40˚, accelerating voltage of 15kv, and a 300-second counting time to increase sensitivity to a detection limit of about 0.03 percent weight PbO.

Five millimeter-diameter chips from each of the five samples from each study sites were subsampled and turned into polished cross-sections. A JEOL superprobe then acquired BSE imagery at a scale of 1000x with a cross-sectional area of 2 mm^2 for each of the five samples. Using methods detailed previously (Dorn 1995; Gordon and Brady 2002), digital image processing of the BSE imagery measures porosity of the weathering rind. The porosity includes intra-mineral pores and pores along mineral-grain boundaries. Though porosity data are calculated to hundredths of a percent using Image J software, a conservative solution in dealing with different pore types is to round off to the nearest tenth of a percent.

A separate experiment was carried out at the Middle Palisade Glacier, California. A ceramic plate was abraded with coarse sandpaper and then

covered with a thin layer of epoxy mixed with bentonite clay, that was then polished with 0.1μm aluminum paste. The ceramic plate was then placed underneath the glacier by fixing it to bedrock. The plate was retrieved after five years for study with electron microscopy to examine any changes.

Results

Despite the appearance of "fresh" rock surfaces with glacially polished surface textures, all samples from all six sites (Table 1) showed some evidence of rock-surface alteration, ranging from mineral decay to the accretion of different types of rock coatings when viewed at micrometer and nanometer scales. The results that follow are preliminary in that they represent the analysis of only a few samples. However, these results illustrate a variety of alteration processes at the retreating margins of glaciers.

Case Hardening of Weathering Rinds

Case hardening necessarily involves two different processes: alteration and dissolution of minerals beneath the surface in a weathering rind; and the accumulation of an indurating agent at the rock surface that can hold the decayed material in place. Three types of hardening agents were found. Silica glaze (Figure 2) and manganiferous rock varnish (Figure 3) formed micron-scale indurating agents. Thin silica glaze (e.g., Figure 2) was much more common as a case-hardening agent at all sites, while rock varnish acted as an indurating agent only at the Bungar Hills and Greenland sites. In addition, iron translocated into the Bungar Hills sample and impregnated the weathering rind to a depth of about 0.25 mm (Figure 4).

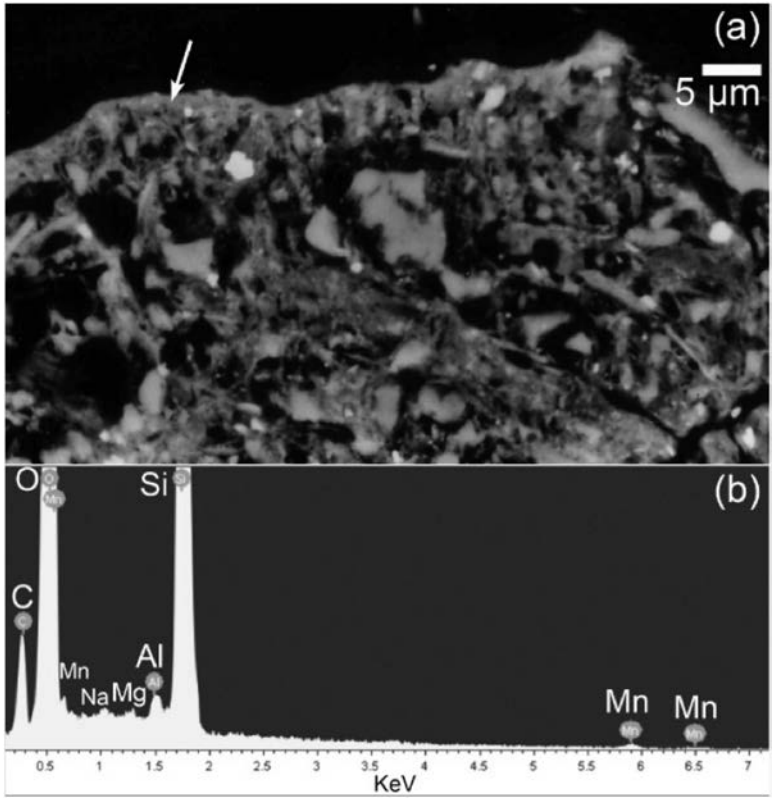

Figure 2.—(a) BSE image of a silica glaze with trace amounts of Na, Mg, Al, and Mn that indurates a weathering rind at the Franz Josef Glacier. The white arrow identifies the location of the EDS analysis shown in image (b). Starting out as schist, the weathering rind contains abundant porosity and the alteration products of mineral decay.

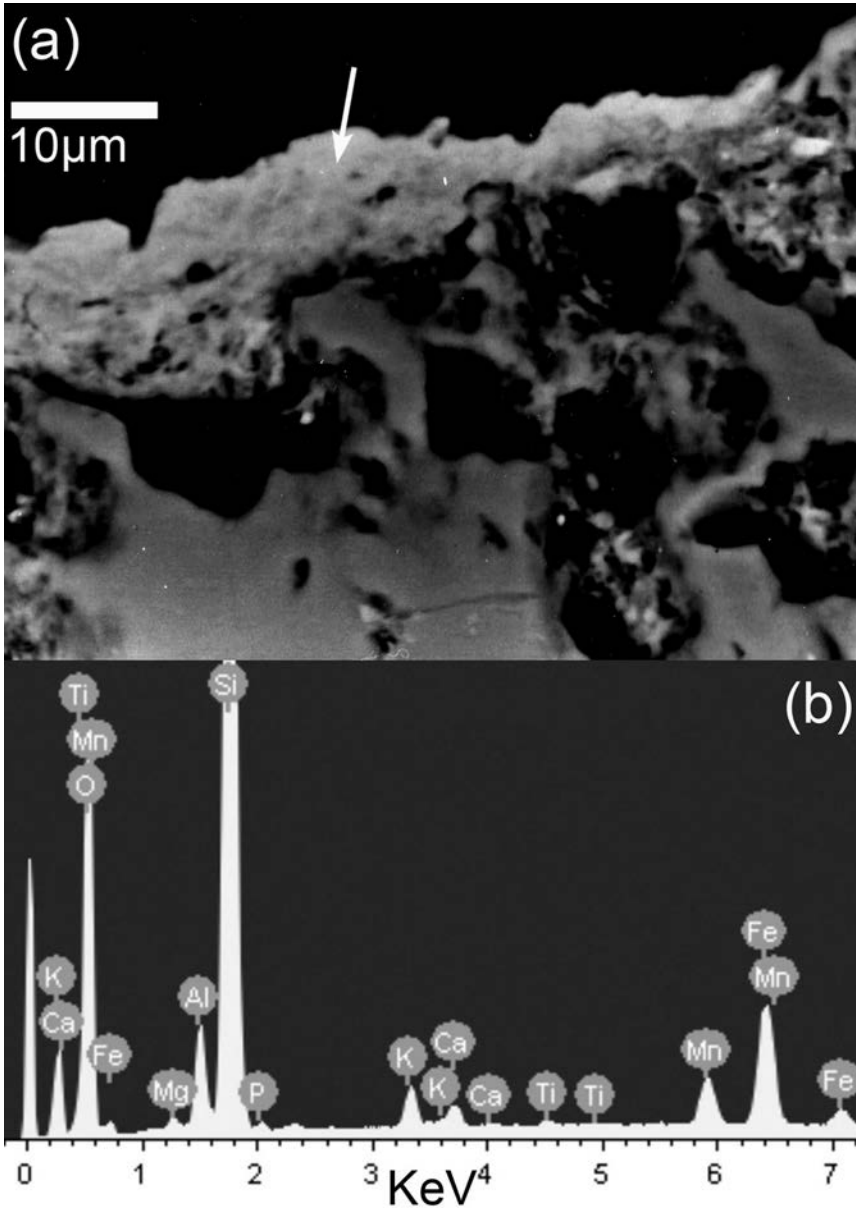

Figure 3.—(a) BSE image of a rock varnish indurating a weathering rind at the Bunger Hills, Antarctica. The white arrow identifies the location the EDS analysis shown in image (b). Starting out as a quartz monzonite, the weathering rind contains abundant porosity in the host quartz mineral.

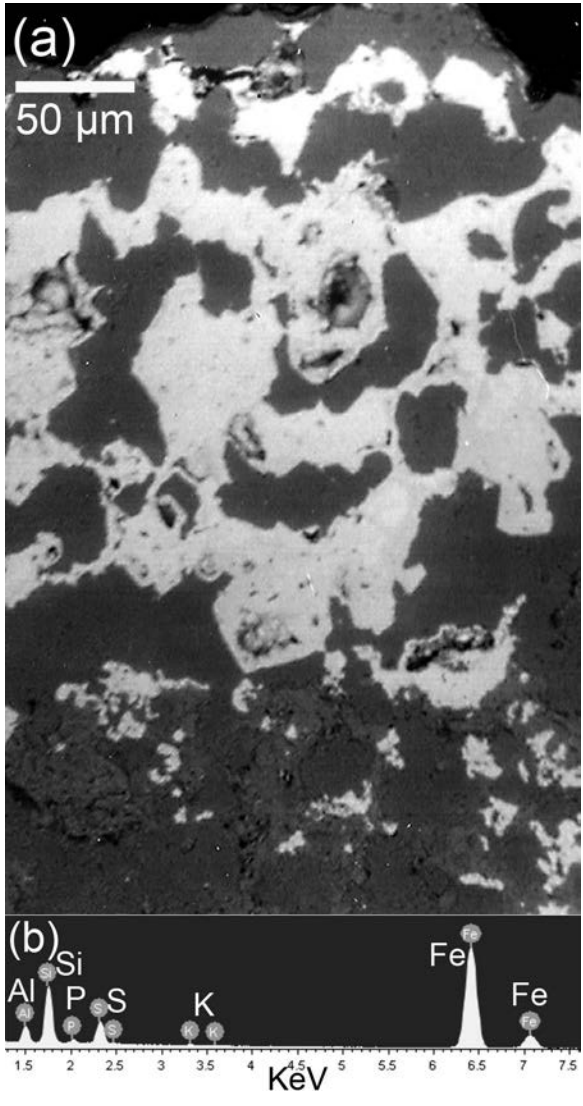

Figure 4.—The Bungar Hills, Antarctica, samples contain a thick iron-rich case hardening of the weathering rind. (a) BSE image of the outer 0.3 mm of granodiorite where pore spaces in the weathering rind have been filled in with iron with minor amounts of aluminum, silicon, phosphorus, sulfur and potassium. (b) This EDS analysis is representative of other EDS measurements of this fairly homogeneous iron-rich case hardening.

Porosity of Weathering Rinds

BSE imagery of case hardening (Figures 2a and 3a) also clearly reveals the presence of rock decay in weathering rinds. Digital image processing of 2 mm^2 of BSE imagery for each of the five samples collected from the six different sites provides a quantitative understanding of the dissolution—all in weathering rinds underneath glacially polished surface textures. The results

reveal considerable variability (Table 2). Still, these findings show that none of the analyzed rocks are truly "fresh" or "unaltered rock."

Table 2.—Total porosity in 2 mm^2 of weathering rinds of glacially polished rocks at the retreating margin of six glaciers.

Glacier	Rock Type	Surface	Percent porosity in weathering rinds of the five samples
Athabascia Glacier, Canada	limestone with silicified nodules	bedrock	0.5%, 1.3%, 2.2%, 2.9%, 4.0%
Bunger Hills, Antarctica	quartz monzonite	boulders	3.5%, 4.4%, 4.9%, 5.2%, 7.1%
Franz Josef Glacier, New Zealand	schist	boulders	0.3% 0.6%, 0.6%, 1.1%, 1.5%
Greenland outlet glacier	gneiss	boulders	2.0%, 2.7%, 3.3%, 4.5%, 4.8%
Ngozumpa Glacier, Nepal	gneiss	boulders	0.6%, 0.7%, 0.7%, 0.9%, 0.9%
Middle Palisade Glacier, USA	granodiorite	bedrock	0.2%, 0.2%, 0.5%, 1.1%, 3.6%

Lead Contamination

Initial EDS analyses of two sites revealed detectable lead concentrations in the surface-most layer of rock varnishes: the Greenland outlet glacier and the Middle Palisade Glacier. Figure 5 exemplifies WDS microprobe profiles from the surface down into varnish where lead abundance falls to background levels beneath the upper micron. While most of the lead appears to be too dispersed to image even with HRTEM, a few cases exist where the lead appears to be concentrated in <10 nm sized particles (Figure 6).

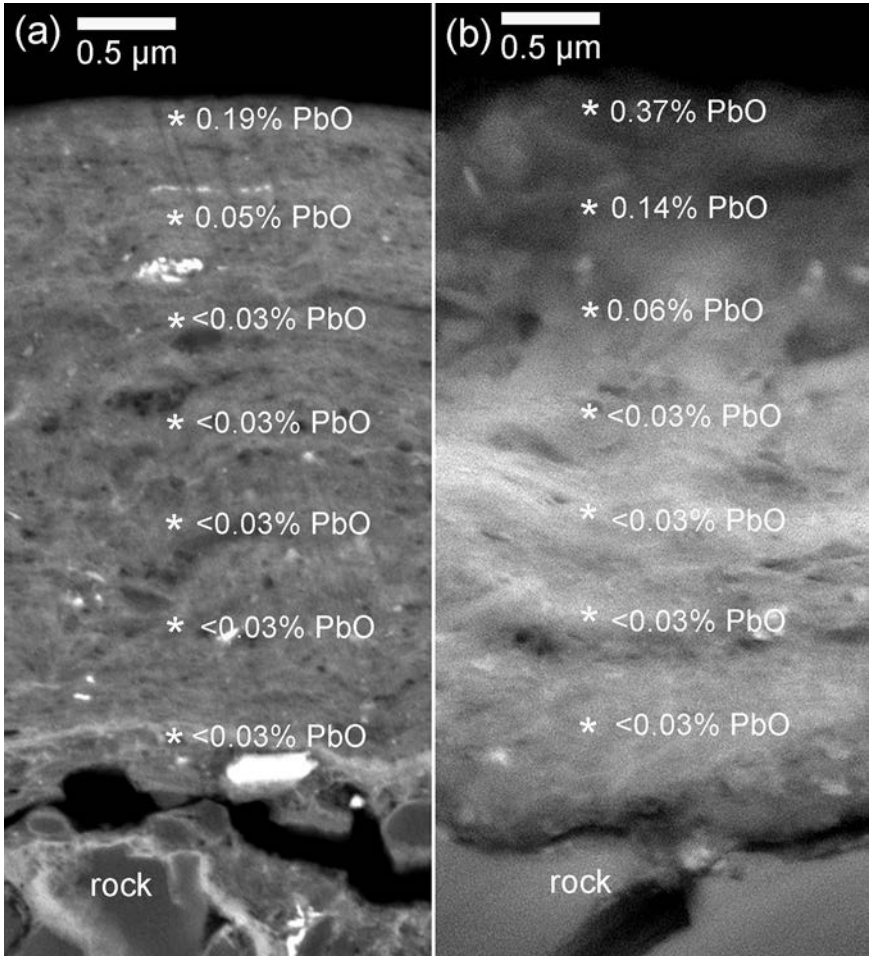

Figure 5.—BSE images of cross-sections of rock varnishes where the surface most layer is contaminated with lead. Each WDS measurement point is about 0.5 µm apart, and this means that these is spatial overlap in the focused beam analyses. Less than 0.03% lead is background, below the limit of detection. (a) Greenland outlet glacier sample; (b) Middle Palisade Glacier sample.

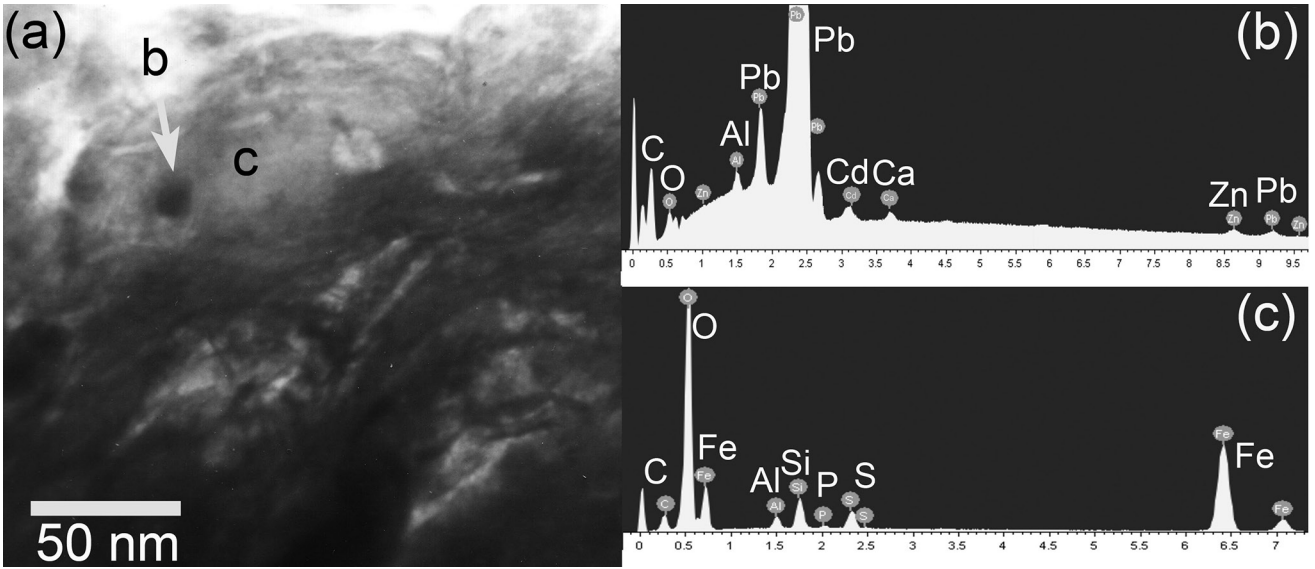

Figure 6.—(a) HRTEM image and associated EDS analyses (b, c) of a lead-rich particle surrounded by an iron hydroxide-rich portion of varnish from the Middle Palisade Glacier. In image (a), the arrow from b to the Pb-rich particle identifies the location of the EDS analysis (b), while the letter c identifies the location of the EDS analysis of the surrounding Fe-rich varnish.

A ceramic plate placed beneath the Middle Palisade Glacier formed rock varnish within five years (Figure 7). The elemental chemistry of this rock varnish, as analyzed by EDS, is the same as varnish occurring on boulders exposed at the glacier margin. A few nanoscale spots on rock varnish revealed the presence of high lead abundances, but only at the scale of what appears to be <50 nm. Erosional striations caused by the movement of particles over the ceramic plate appear to stand out as positive relief features in Figure 7. This is because the very surface of the covered ceramic plate exposed to the glacier was composed of a mixture of epoxy and bentonite clay that was then polished. Movement of particles over this soft surface resulted in a "plowing" action that generated the positive relief seen in the Figure 7a.

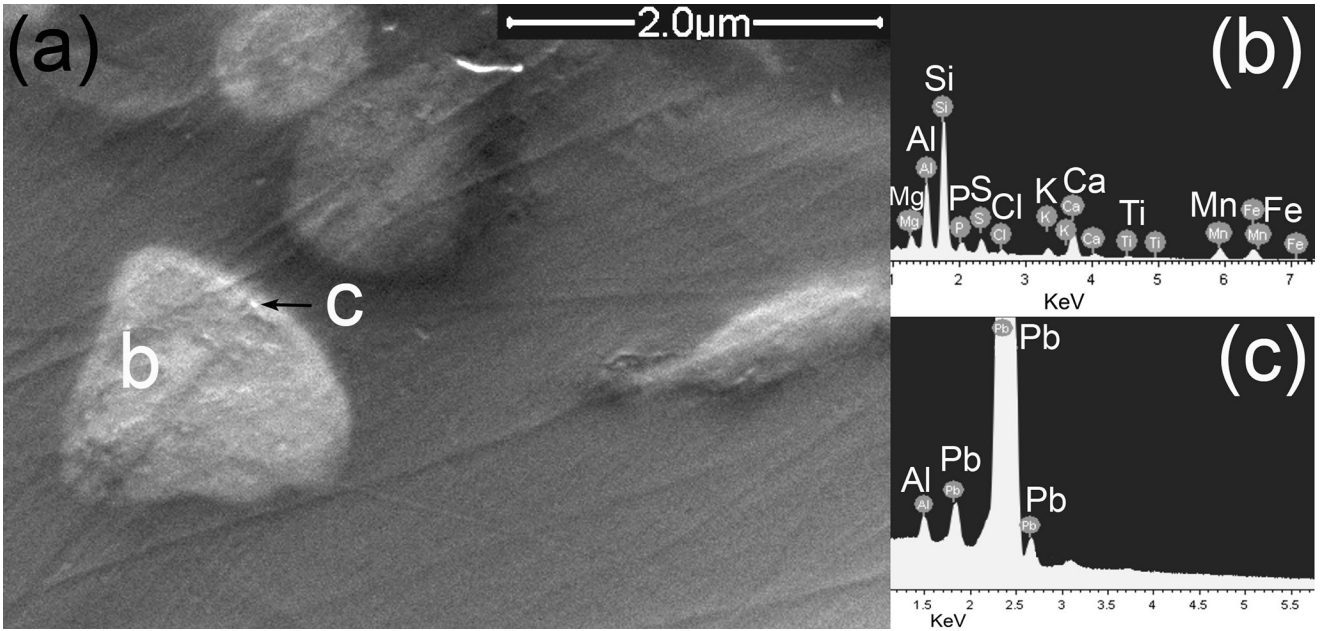

Figure 7.—A ceramic plate covered with an epoxy-bentonite polished covering was placed underneath the Middle Palisade Glacier, California, for five years. (a) SE image of a portion of the ceramic plate. The letter b indicates the location of the EDS analysis shown in image (b) with a spectra typical of rock varnish. The letter c identifies a spot on the varnish that is greatly enriched in lead, as shown in image (c).

Fungal Mat

All of the glacially polished boulders from the Franz Josef Glacier hosted fungal mats (e.g., Figure 8). These mats were not uniform over the boulders and were typically less than 2 mm in diameter. Irregularly spaced portions of the fungal mats contained iron- and clay-rich portions that have an elemental chemistry similar to Mn-poor/Fe-rich rock varnish (Figure 8b and 8c). No other sites hosted fungal mats.

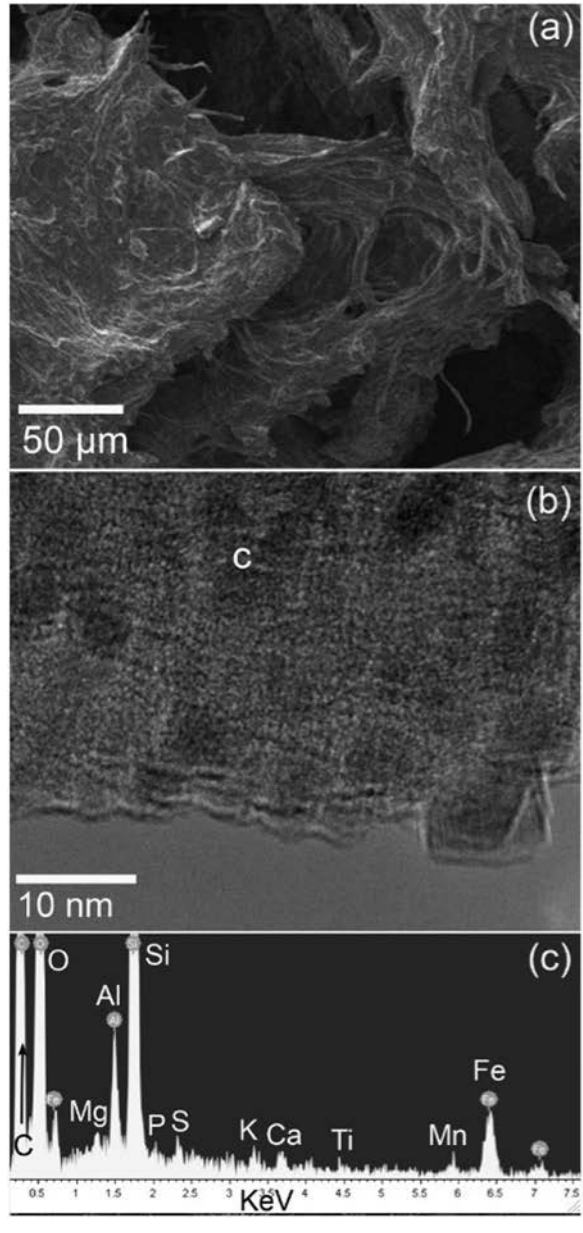

Figure 8.—Fungal mat growing on a boulder at the margin of the Franz Josef Glacier. (a) SE image (b) HRTEM image of the contact between fungi and the underlying plagioclase mineral. (c) EDS analysis acquired from the letter c in image (b). This EDS signature is similar to Mn-poor rock varnish, with the exception of the strong carbon peak.

Silica Glaze

Silica glaze is the most common type of rock coating found at the six sampling sites. Most of the silica glaze consists of micron-thin coatings (e.g., Figure 2). However, thicker silica glazes did occur at the Bungar Hills, Greenland outlet, and Ngozumpa Glacier sites. Figure 9 includes the two observed textures of silica glaze: finely laminated and more massive in BSE appearance. While the EDS image in Figure 9b is for a finely laminated texture, this EDS spectra is typical of most of the silica glazes observed.

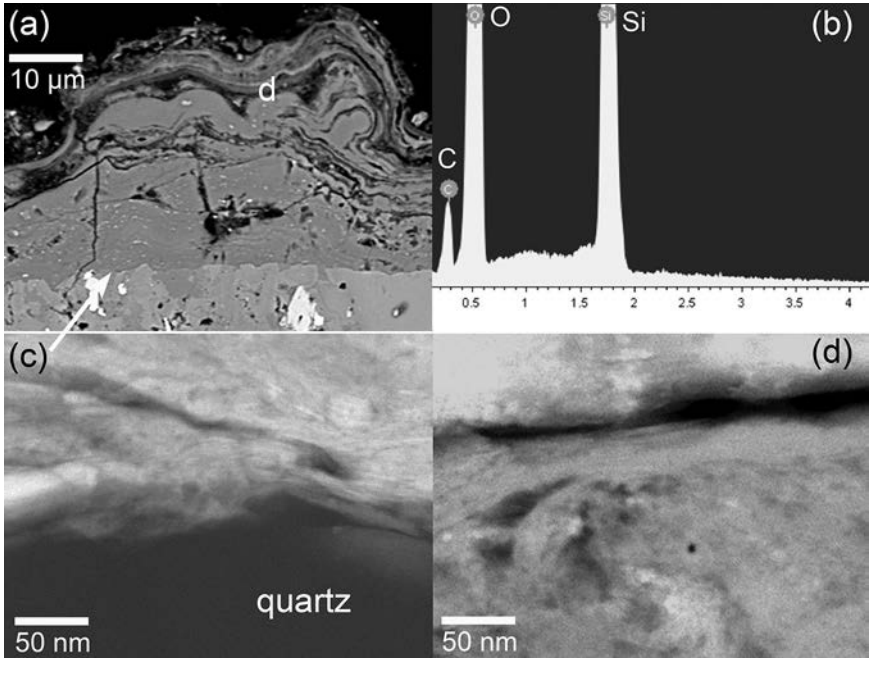

Figure 9.—Silica glaze from the Ngozumpa Glacier, Nepal. (a) BSE image showing two textures of silica glaze accreted on the underlying glacially polished surface. The upper texture shows fine laminations, while the lower texture appears more massive. (b) EDS of the finely laminated texture. (c) Higher resolution BSE image (from the arrow tip in image (a) of the contact between quartz in the underlying rock and the overlying silica glaze. (d) A higher-resolution BSE image at the location identified with a d in image (a). Note the nanoscale laminations in the upper half of image d and a more chaotic texture underneath at the nanoscale. This more chaotic texture has a more massive appearance at lower resolutions, such as image (a).

Mg-rich Coating on Glacial Polish

Glacially polished limestone (with silica nodules) sampled from underneath the Athabasca Glacier hosted two types of rock coatings not reported previously in scholarship. One coating appears to be an iron film, but with a very strong enrichment in magnesium (Figure 10). This interpretation is based on EDS spectra (Figures 10c and 10d) that were quite similar in different analyses of the coating. If one ignores the strong Mg (and Ca) peak, the rest of the EDS spectra would be similar to a Fe-rich/Mn-poor rock varnish that contains abundant clay minerals (strong Al and Si peaks). However, the very strong Mg and moderately high Ca peaks have not been found previously in other examples of Fe-rich varnishes. One speculative interpretation is that the very strong peak of Mg stands out as an anomaly that could be explained by crystals of mixed magnesite ($MgCO_3$) and ankerite [$Ca(Fe,Mg,Mn)(CO_3)_2$] that could explain the very high Mg peak, the iron, and also the layered texture. The desiccation cracks (Figures 10a and c) cracking could be an artifact of the carbon coating process, or it could be an original surface micromorphology. The pedestal in Figure 11b with similar sized peaks for Ca and Mg, however, could be dolomite.

A glacially polished silicified nodule collected from underneath the Athabasca Glacier also showed the presence of the Mg-rich coating (Figure 11a) with an EDS spectra (Figure 11b) similar to the coating observed on the limestone (Figure 10). There are two differences: the coating exists only as a micron-scale patch (see letter b in Figure 11a); and the relative height of the calcium peak is much less than in Figure 10. In addition, pedestals (Figure 11c) with an EDS spectra similar to manganiferous rock varnish (Figure 11d) dot the surface of the silicified nodules. The lower-resolution image 11a identifies one of the Mn-rich pedestals with the letter c, and that pedestal is shown with nanoscale detail in Figure 11c.

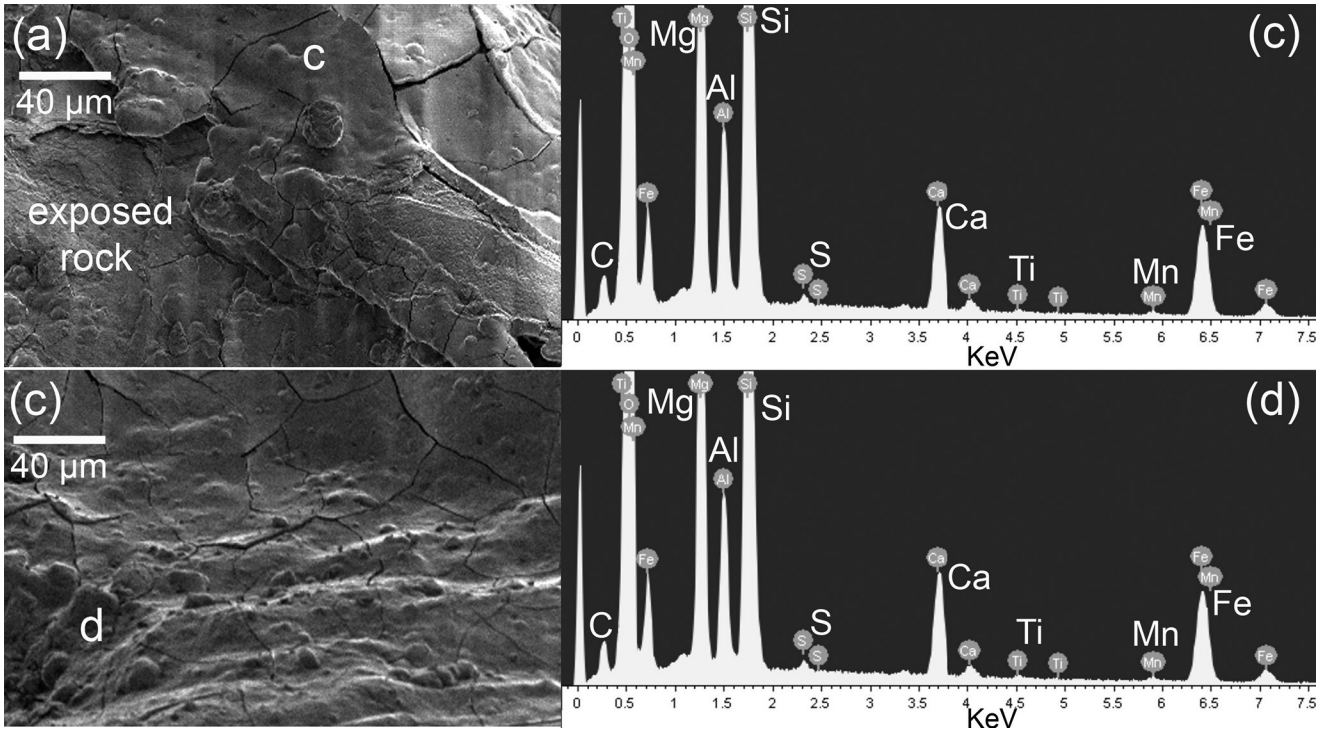

Figure 10. —Magnesium-rich rock coating on limestone collected from underneath the Athabasca Glacier. SE images (a) and (c) show fairly smooth textures of the coating that appears to have desiccation cracks. Image (a) shows a bit of the underlying limestone rock exposed when the coating flaked off during sampling. The letters c and d in the SE images identify the locations of the EDS analyses in images (c) and (d).

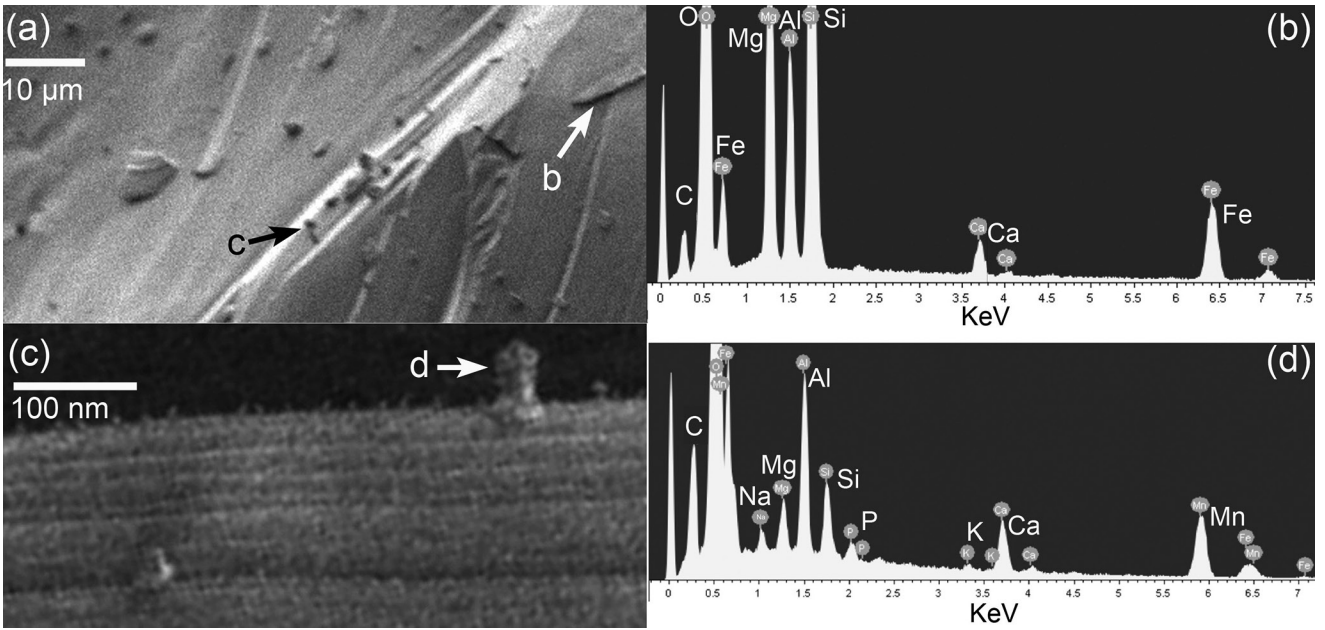

Figure 11.—Glacially polished silicified nodule underneath the Athabasca Glacier showed growths of two types of rock coatings. (a) SE image that shows a micron-scale coating (see b and associated white arrow) and also sub-micron accretions (see c and associated black arrow) (b) EDS analysis of the coating identified by the b arrow in image (a). (c) Higher-resolution SE image of the location identified by the c black arrow in image (a). (d) EDS analysis of the pedestal identified by the white d and arrow in image (c).

Discussion

Electron microscope examination of recently exposed boulders and bedrock—all with a surface texture of glacially polished rock from six different arctic and alpine glacier margins—reveals the presence of several different rock coatings and the development of weathering rinds on all studied surfaces. This section links these initial results of this pilot study to prior scholarship.

Rock Surface Decay

There exists some potential of these preliminary findings to impact research on the timing of late-Holocene glacial events in California, Oregon, Washington, and Alaska. At issue is the most recent of glacial advances, the late Holocene (Porter and Denton 1967; Scuderi 1987), as well as advances and retreats of small glaciers in the twentieth century (Dyurgerov and Meier 2000), since weathering rinds have been used to generate relative ages throughout the Pacific Coast region (e.g., Porter 1975).

Paraglacial rock decay can progress rapidly in both periglacial and paraglacial settings (Dixon et al. 1984; Ballantyne and Benn 1994; Thorn et al. 2001; Dixon et al. 2002; French and Guglielmin 2002; Dixon and Thorn 2005; Thorn et al. 2006; Dixon 2013) by both abiotic decay processes (Anderson et al. 2000) and microorganism-generated decay (Etienne 2002; Etienne and Dupont 2002; Guglielmin et al. 2005; Borin et al. 2010). Such rapid decay has been also documented physically through microrelief measurements (Dąbski 2015).

Thus, the presence of weathering rinds (Figures 2 and 3) with varying degrees of porosity (Table 2) should not be a surprise, even if no prior rock-surface porosity data are available at the retreating margins of glaciers. What cannot be discerned, however, is whether dissolution and mineral alteration took place: (a) subglacially before, during, or after glacial polishing of the studied surfaces; (b) on boulder perimeters during glacial transport; or (c) on the margins of the retreating glaciers. There is no way to rule out alteration in any of these contexts.

What is clear from these results, however, is that those who use weathering-rind thicknesses or Schmidt hammer testing as an indicator of time since deglaciation (Guglielmin et al. 2012; Dabski and Tittenbrun 2013; Reznichenko et al. 2016; Zasadni and Kłapyta 2016; Mills et al. 2017) can no longer assume an initial condition of "fresh rock" with no prior decay. Table 2 reveals the presence of porosity in all weathering rinds, that in

turn can potentially influence both weathering rind appearance and also Schmidt hammer testing. Table 2 reveals that porosity varies considerably from boulder to boulder or bedrock surface to bedrock surface. This initial variability thus creates an additional uncertainty factor for studies involving weathering-rind thickness and Schmidt Hammer testing.

Lead Contamination

Lead pollution is a global issue that results when micrometer-scale and nanoscale lead particles get transported via rain drops, and hence frequently are found in soils and plants near roadways (Motto et al. 1970; Patterson 1980; Agrawal et al. 1981; Newsome et al. 1997) and in regolith pores near highways (Fein et al. 1999). Although lead pollution concentrates near locations of emission such as highways and smelters, lead distribution occurs globally through atmospheric processes as evidenced by lead pollution occurrences in Danish bogs (Andersen 1994) and ice (Boutron et al. 1994) distant from emission sources.

Oxides and hydroxides of iron and manganese scavenge lead (Jenne 1968; Gulson et al. 1992; Coston et al. 1995; Dong et al. 2002; Adams et al. 2009). This basic observation led to an investigation of whether lead contaminates the surface-most layer in rock varnish with the basic finding as follows:

> Lead accumulates in rock varnishes and dust films on desert surfaces. Electron microprobe profiles reveal that lead is a contaminant in the uppermost surfaces of rock varnishes, but these concentrations drop to background levels below the very surface of natural rock coatings that have formed since lead additives were introduced into gasoline in 1922. (Dorn, 1998: 139)

Since this initial finding, lead emitted by automobile exhaust has been found in the surface-most layer of varnish (Fleisher et al. 1999), including in eastern California areas distant from cities (Broecker and Liu 2001). Similarly, other research has documented contamination by lead and other heavy-metal contaminants in the surface-most layer of rock varnish (Thiagarajan and Lee 2004; Hodge et al. 2005; Wayne et al. 2006; Spilde et al. 2007; Nowinski et al. 2010; Hoar et al. 2011; Nowinski et al. 2012; Spilde et al. 2013).

Nanoscale iron and manganese are likely the key to lead fixation in surficial rock varnish. As lead diffuses into varnish (Figure 5), recently deposited varnish experiences ongoing instability at the nanoscale, as oxides

and hydroxides of iron and manganese move a few nanometers from bacterial casts into clay minerals (Dorn 2013; Krinsley et al. 2013; Krinsley et al. 2017). Atmospheric fallout of lead that encounters rock varnish (Figures 6 and 7) interacts with this ongoing nanoscale instability as nanoscale Mn-Fe particles cement clay minerals to form varnish (Dorn 1998; Dorn 2007). The lead is then scavenged by the precipitating nanoscale Mn-Fe particles.

Three new findings regarding lead interaction with rock varnish are new to this study. First, the ceramic plate study (Figure 7) documents that lead adsorption can occur in as little as five years and in subglacial settings. Second, lead is contaminating varnish even in remote environments like Greenland (Figure 5). Third, presence of lead as a twentieth-century contaminant on developed weathering rinds supports the observation of recent exposure of glacial boulders with already-developed weathering rinds.

Rock Coatings

While many think of rock coatings as a subaerial accretion, they can also have a subglacial origin as evidenced by Mn-rich birnessite subglacial coatings of the Jackson Glacier in Montana and Khumbu Glacier in Nepal (Potter and Rossman 1979), as well as observations of ferromanganese rock varnish formation in Norway (Whalley et al. 1990). Silica glaze formed subglacially may result from processes associated with "sliding ice" (Hallet 1975). Iron films have been reported in association with subglacial meltwaters (Anderson and Sollid 1971; Whalley 1984; Drewry 1986). Subglacial carbonate coatings (Hallet 1976; Bernard 1979; Souchez and Lemmens 1985; Liu et al. 2005) can be deposited in microlaminations and also cementing rock fragments (Carter et al. 2003; Liu et al. 2005). Microscopic observations indicate textures associated with cryogenic calcite crystallization (Sharp et al. 1990) and perhaps cryogenic involvement in iron and silica precipitation as well (Vogt 1990; Vogt and Corte 1996). Given this prior scholarship, the rock coatings observed in Figures 2 through 11 could be inherited from a subglacial environment or could be forming at the retreating margins of glaciers.

Several new observations about rock coatings emerged in this study. First, fungi in a paraglacial setting next to the Franz Josef Glacier in New Zealand are able to generate elemental constituents similar to Mn-poor/Fe-rich rock varnish within the mat (Figure 8). Second, I am unaware of an elemental signature for the rock coatings observed underneath the Athabasca Glacier, Canada (Figure 10 and 11b), with such a strong Mg peak combined with elements similar to Mn-poor rock varnish. Third, the nanoscale growth

form as observed in Figure 11c with an elemental chemistry of rock varnish (Figure 11d) appears similar to budding bacteria cast forms that are implicated in varnish formation (Dorn and Oberlander 1982) and occur within varnishes formed along the Erie Canal (Krinsley et al. 2017). Third, silica glaze (Figures 2 and 9) is the most common paraglacial rock coating observed in the six paraglacial settings studied here. Fourth, silica glaze, rock varnish, and iron can also act as indurating case-hardening agents (Dorn 2004) on the retreating margins of glaciers.

Conclusions

The general notion that physical processes of rock decay dominate over chemical and biochemical processes of rock decay has long been debunked for cold climates, including paraglacial settings (Pope et al. 1995). In these environments, soil scientists, physical geographers, surficial geologists, and Quaternary scientists often study weathering rinds in paraglacial settings. A common assumption made in these studies is that abrasive processes such as glacial polishing removes pre-existing rock decay and exposes a "fresh surface."

Micrometer and nanometer-scale examination of glacially polished samples exposed at the retreating margins of six glaciers revealed the presence of weathering-rind porosity in all samples and in highly variable amounts. This is a preliminary finding, because of the relatively low number of samples analyzed. Also, there is a need to analyze in detail the status of weathering of clasts still embedded in the glacier prior to deposition. Still, the presence of weathering-rind porosity suggests a possible need for establishing an initial state of rock decay before interpreting results of Schmidt Hammer testing or weathering-rind measurements on glacial moraines.

Natural coatings are analogous to cumulic soils in that they record environmental processes occurring at the earth's surface. Glacially polished rock exposed at the retreating margins of the Athabasca Glacier in Canada, Bunger Oasis of Antarctica, Franz Josef Glacier in New Zealand, a Greenland outlet glacier, Ngozumpa Glacier in Nepal, and the Middle Palisade Glacier in California display a range of rock coatings, including a newly type of Mg-rich coating, iron films, rock varnish, fungal mats, and silica glaze as the most common coating. Silica glaze, rock varnish, and iron film constituents are able to impregnate the weathering rind and generate a case-hardening effect. Although samples were collected within a few meters from ice on glacially polished surfaces, rock coatings occurred on all surfaces rang-

ing from micrometer- to millimeters-scale in size. Ceramic plates placed in contact with the Middle Palisade Glacier in California developed rock varnish with an elemental composition similar to varnish found on nearby exposed glacially polished rock.

Because manganiferous rock varnish is a known scavenger of heavy metals, including lead, coatings exposed by ongoing glacial ablation are able to record anthropogenic air pollution. Evidence of twentieth- and twenty-first-century anthropogenic contamination from lead occurred in the top micrometer of rock varnish collected from recently deglaciated boulders exposed on a medial moraine of a Greenland ice sheet outlet glacier, from recently deglaciated boulders found on the margin of the Middle Palisade Glacier in California, and also rock varnish formed on a ceramic plate placed underneath the Middle Palisade Glacier for five years. Thus, an Anthropocene signal of lead pollution contaminates rock surfaces on the retreating margins of even remote glaciers and ice sheets.

Given the long history of research into glacial advances in the Pacific Coast region (e.g., Kesseli 1941; Whelan and Bach 2017), and since a number of retreating glaciers now exist, we hope that findings of this pilot research might generate further research within the region.

Acknowledgments

This research was made possible, in part, by sabbatical support from Arizona State University. Antarctic samples were supplied by Ran Gerson. Greenland samples were supplied by Barbara Murphy.

Literature Cited

Adams, J. P., R. Kirst, L. E. Kearns, and M. P. S. Krekeler 2009. Mn-oxides and sequestration of heavy metals in a suburban catchment basin of the Chesapeake Bay watershed. *Environmental Geology* 58:1269–1280.

Agrawal, Y. L., M. P. Patel, and S. S. Merh 1981. Lead in soils and plants: its relationship to traffic volume and proximity to highway (Lalbag, Baroda city). *International Journal of Environmental Studies* 16:222–224.

Anders, A. M., R. S. Sletten, L. A. Derry, and B. Hallet 2003. Germanium/silicon ratios in the Copper River Basin, Alaska: Weathering and partitioning in periglacial versus glacial environments. *Journal of Geophysical Research: Earth Surface* 108(F1):DOI: 10.1029/2003JF000026.

Andersen, S. T. 1994. History of the terrestrial environment in the Quaternary of Denmark. *Bulletin of the Geological Society of Denmark* 41:219–228.

Anderson, J. L., and J. L. Sollid 1971. Glacial chronology and glacial geomorphology in the marginal zones of the glaciers, Midtadlsbreen and Nigardsbreen, South Norway. *Norsk Geografisk Tidsskrift* 25:1–35.

Anderson, S. P. 2007. Biogeochemistry of glacial landscape systems. *Annual Review Earth and Planetary Sciences* 35:375–399.

Anderson, S. P., J. I. Drever, C. D. Frost, and P. Holden 2000. Chemical weathering in the foreland of a retreating glacier. *Geochimica et Cosmochimica Acta* 64:1173–1189.

Ballantyne, C. K., and D. I. Benn 1994. Paraglacial slope adjustment and resedimentation following recent glacier retreat, Fåbergstølsdalen, Norway. *Arctic, Antarctic, and Alpine Research* 26:255–269.

Bernard, H. 1979. Subglacial regelation water film. J*ournal of Glaciology* 23:321–334.

Bhatia, M. P., E. B. Kujawinski, S. B. Das, C. F. Breier, P. B. Henderson, and M. A. Charette 2013. Greenland meltwater as a significant and potentially bioavailable source of iron to the ocean. *Nature Geoscience* 6:274–278.

Borin, S., S. Ventura, F. Tambone, et al. 2010. Rock weathering creates oases of life in a High Arctic desert. Environmental microbiology. *Environmental Microbiology* 12:293–303.

Boutron, C. F., J.-P. Candelon, and S. Hong 1994. Past and recent changes in the large-scale tropospheric cycles of lead and other heavy metals as documented in Antarctic and Greenland snow and ice: A review. *Geochimica et Cosmochimica Acta* 58:3217–3225.

Boyd, E. S., T. L. Hamilton, J. R. Havig, M. L. Skidmore, and E. L. Shock 2014. Chemolithotrophic primary production in a subglacial ecosystem *Applied and environmental microbiology* 80:6146–6153.

Broecker, W. S., and T. Liu 2001. Rock varnish: recorder of desert wetness? *GSA Today* 11 (8):4–10.

Brown, G. H. 2002. Glacier meltwater hydrochemistry. *Applied Geochemistry* 17:855-883.

Burbank, D. W., and K. J. Cheng 1991. Relative dating of Quaternary moraines, Rongbuk Valley, Mount Everest, Tibet: implications for an ice sheet on the Tibetan Plateau. *Quaternary Research* 36:1–18.

Burke, R. M., and P. W. Birkeland 1979. Reevaluation of multiparameter relative dating techniques and their application to the glacial sequence along the eastern escarpment of the Sierra Nevada, California. *Quaternary Research* 11:11–51.

Carter, C. L., D. P. Dethier, and R. L. Newton 2003. Subglacial environment inferred from bedrock-coating siltskins, Mendenhall Glacier, Alaska, USA. *Journal of Glaciology* 49:568–576.

Chinn, T. J. H. 1981. Use of rock weathering-rind thickness for Holocene absolute age-dating in New Zealand. *Arctic and Alpine Research* 13:33–45.

Colman, S. M., and K. L. Pierce 1981. Weathering rinds on andesitic and basaltic stones as a Quaternary age indicator, western United States. *U.S. Geological Survey Professional Paper* 1210:1–56.

———. 1986. Glacial sequence near McCall Idaho: Weathering rinds, soil development, morphology, and other relative-age criteria. *Quaternary Research* 25:25–42.

Coston, J. A., C. C. Fuller, and J. A. Davis 1995. Pb2+ and Zn2+ adsorption by a natural aluminum-bearing and iron-bearing surface coating on an aquifer sand. *Geochimica et Cosmochimica Acta* 59:3535–3547.

Dąbski, M. 2015. Application of the Handysurf E-35B electronic profilometer for the study of weathering micro-relief in glacier forelands in SE Iceland. *Acta Geologica Polonica* 65:389–401.

Dąbski, M., and A. Tittenbrun 2013. Time-dependent surface deterioration of glacially abraded basaltic boulders by Fláajökull, SE-Iceland. *Jökull* 63:55–70.

Dixon, J. C. 2013. Chemical weathering in cold climates. In ed. G. Pope, *Treatise on Geomorphology, vol. 4*, pp. 245–257. San Diego: Academic Press.

Dixon, J. C., and C. E. Thorn 2005. Chemical weathering and landscape development in alpine environments. *Geomorphology* 67:127–145.

Dixon, J. C., C. E. Thorn, and R. G. Darmody 1984. Chemical weathering processes on the Vantage Peak nunatak, Juneau Icefield, southern Alaska. *Physical Geography* 5:111–131.

Dixon, J. C., C. E. Thorn, R. G. Darmody, and S. W. Campbell 2002. Weathering rinds and rock coatings from an Arctic alpine environment, northern Scandinavia. *Geological Society of America Bulletin* 114:226–238.

Dong, D., X. Hua, and L. Zhonghua 2002. Lead adsorption to metal oxides and organic material of freshwater surface coatings determined using a novel selective extraction method. *Environmental Pollution* 119:317–321.

Dorn, R. I. 1995. Digital processing of back-scatter electron imagery: A microscopic approach to quantifying chemical weathering. *Geological Society of America Bulletin* 107:725–741.

———. 1998. *Rock coatings*. Amsterdam: Elsevier.

———. 2004. Case hardening. In ed. A. S. Goudie, *Encyclopedia of Geomorphology*, pp. 118–119. London: Routledge.

———. 2007. Rock varnish. In eds. D. J. Nash and S. J. McLaren, *Geochemical Sediments and Landscapes*, pp. 246–297. London: Blackwell.

———. 2013. Rock coatings. In ed. G. A. Pope, *Treatise on Geomorphology*, vol. 4, pp. 70–97. San Diego: Academic Press.

Dorn, R. I., and T. M. Oberlander 1982. Rock varnish. *Progress in Physical Geography* 6:317–367.

Drewry, D. J. 1986. *Glacial geologic processes*. London: Arnold.
Dyurgerov, M. B., and M.F . Meier 2000. Twentieth century climate change: evidence from small glaciers. *Proceedings of the National Academy of Sciences* 97:1406–1411.
Etienne, S. 2002. The role of biological weathering in periglacial areas: a study of weathering rinds in south Iceland. *Geomorphology* 47:75–86.
Etienne, S., and J. Dupont 2002. Fungal weathering of basaltic rocks in a cold oceanic environment (Iceland): comparison between experimental and field observations. *Earth Surface Processes and Landforms* 27:737–748.
Fairchild, I. J., J. A. Killawee, M. J. Sharp, B. Spiro, B. Hubbard, and R. D. Lorrain 1999. Solute generation and transfer from a chemically reactive alpine glacial-proglacial system. *Earth Surface Processes and Landforms* 24:1189–1211.
Fein, J. B., P. V. Brady, J. C. Jain, R. I. Dorn, and J. Lee 1999. Bacterial effects on the mobilization of cations from a weathered Pb-contaminated andesite. *Chemical Geology* 158:189–202.
Fleisher, M., T. Liu, W. Broecker, and W. Moore 1999. A clue regarding the origin of rock varnish. *Geophysical Research Letters* 26 (1):103–106.
Foulkes, C., and S. Harrison 2014. Evaluating the Schmidt hammer as a method for distinguishing the relative age of late Holocene moraines: Svellnosbreen, Jotunheimen, Norway. Geografiska Annaler: Series A, *Physical Geography* 96:393–402.
French, H. M., and M. Guglielmin 2002. Observations on granite weathering phenomena, Mount Keinath, Northern Victoria Land, Antarctica. *Permafrost and Periglacial Processes* 13:231–236.
Gordon, S. J., and P. V. Brady 2002. In situ determination of long-term basaltic glass dissolution in the unsaturated zone. *Chemical Geology* 90:115–124.
Graly, J. A., N. F. Humphrey, C. M. Landowski, and J. T. Harper 2014. Chemical weathering under the Greenland ice sheet. *Geology* 42:551–554.
Guglielmin, M., N. Cannone, A. Strini, and A. G. Lewkowicz 2005. Biotic and abiotic processes on granite weathering landforms in a cryotic environment, northern Victoria Land, Australia. *Permafrost and Periglacial Processes* 16:69–85.
Guglielmin, M., M. R. Worland, P. Convey, and N. Cannone 2012. Schmidt Hammer studies in the maritime Antarctic: application to dating Holocene deglaciation and estimating the effects of macrolichens on rock weathering. *Geomorphology* 155:34–44.
Gulson, B. L., S. Church, K. Mizon, and A. Meier 1992. Lead isotopes in iron and manganese oxide coatings and their use as an exploration guide for concealed mineralization. *Applied Geochemistry* 7:495–511.
Hallet, B. 1975. Subglacial silica deposits. *Nature* 254:682–683.

———. 1976. Deposits formed by subglacial precipitation of $CaCO_3$. *Geological Society of America Bulletin* 87:1003–1015.

Hoar, K., P. Nowinski, V. F. Hodge, and J. V. Cizdziel 2011. Rock varnish: A passive forensic tool for monitoring recent air pollution and source identification. *Nuclear Technology* 175:351–359.

Humphreys, J., R. Beanland, and P. J. Goodhew 2014. *Electron microscopy and analysis*. Boca Raton, Florida: CRC Press.

Hodge, V. F., D. E. Farmer, T. A. Diaz, and R. L. Orndorff 2005. Prompt detection of alpha particles from Po-210: another clue to the origin of rock varnish? *Journal of Environmental Radioactivity* 78:331–342.

Jenne, E. A. 1968. Controls on Mn, Fe, Co, Ni, Cu and Zn concentrations in soils and water: the significant role of hydrous Mn and Fe oxides. In ed. R. F. Gould, *Trace Inorganics in Water*, pp. 337–387. Washington D.C.: American Chemical Society.

Kaštovská, K., M. Stibal, M. Šabacká, B. Černá, H. Šantrůčková, and J. Elster 2007. Microbial community structure and ecology of subglacial sediments in two polythermal Svalbard glaciers characterized by epifluorescence microscopy and PLFA. *Polar Biology* 30:277–287.

Kesseli, J. E. 1941. Quaternary history of Mono Valley, California. *University of California Publications in Geography* 6:315–362.

Kłapyta, P. 2013. Application of Schmidt hammer relative age dating to Late Pleistocene moraines and rock glaciers in the Western Tatra Mountains, Slovakia. *Catena* 111:104–121.

Krinsley, D., J. Ditto, K. Langworthy, R. I. Dorn, and T. Thompson 2013. Varnish microlaminations: new insights from focused ion beam preparation. *Physical Geography* 34:159–173.

Krinsley, D. H., R. I. Dorn, B. E. DiGregorio, J. Razink, and R. Fisher 2017. Mn-Fe enhancing budding bacteria in century-old rock varnish, Erie Canal, New York. *Journal of Geology* 125:317–336.

Liu, G., R. Luo, J. Cao, and Z. Cui 2005. Processes and environmental significance of the subglacial chemical deposits in Tianshan Mountains. *Science in China Series D: Earth Sciences* 48:1470–1478.

Mahaney, W. C., and L. Keiser 2013. Weathering rinds: unlikely host clasts for evidence of an impact-induced event. *Geomorphology* 184:74–83.

Mahaney, W. C., and S. Schwartz 2016. Paleoclimate of Antarctica reconstructed from clast weathering rind analysis. *Palaeogeography, Palaeoclimatology, Palaeoecology* 446:205–212.

McCarroll, D. 1989. Potential and limitations of the Schmidt hammer for relative-age dating. Field-tests on neoglacial moraines, Jotunheimen, Southern Norway. *Arctic and Alpine Research* 21:268–275.

———. 1994. The Schmidt Hammer as a measure of degree of rock surface weathering and terrain age. In ed. C. Beck, *Dating in exposed and surface contexts*, pp. 29–45. Albuquerque: University of New Mexico Press.

Mills, S. C., T. T. Barrows, M. W. Telfer, and L. K. Fifield 2017. The cold climate geomorphology of the Eastern Cape Drakensberg: A reevaluation of past climatic conditions during the last glacial cycle in Southern Africa. *Geomorphology* 278:184–194.

Mitchell, A. C., M. J. Lafrenière, M. L. Skidmore, and E. S. Boyd 2013. Influence of bedrock mineral composition on microbial diversity in a subglacial environment. *Geology* 41:855–858.

Motto, H. L., R. H. Dines, D. M. Childko, and C. K. Motto 1970. Lead in soils and plants: it relationship to traffic volume and proximity to highways. *Environmental Science and Technology* 4:231–237.

Newsome, T., F. Aranguren, and R. Brinkmann 1997. Lead contamination adjacent to roadways in Trujillo, Venezuela. *Professional Geographer* 49:331–341.

Nowinski, P., V. F. Hodge, and S. Gerstenberger 2012. Application of field portable X-ray fluorescence to the analysis of desert varnish samples in areas affected by coal-fired power plants. *Environmental Chemistry* 9:379–388.

Nowinski, P., V. F. Hodge, K. Lindley, and J. V. Cizdziel 2010. Elemental analysis of desert varnish samples in the vicinity of coal-fired power plants and the Nevada Test Site using laser ablation ICP-MS. *The Open Chemical and Biomedical Methods Journal* 3:153–168.

Patterson, C. C. 1980. An alternative perspective-lead pollution in the human environment: origin, extent and significance. In eds. B. B. Ewing, C. I. Davidson, N. L. Gale, J. M. Hunger, S. Lichtenstein, A. H. Lubin, K. Mahaffey, J. Nriagu, C. C. Patternson, E. A. Pfitzer, R. K. Skogerboe and L. B. Tepper, *Lead in the Human Environment*, pp. 265–349. Washington D.C.: National Academy of Sciences.

Pope, G., R. I. Dorn, and J. Dixon 1995. A new conceptual model for understanding geographical variations in weathering. *Annals of the Association of American Geographers* 85:38–64.

Porter, S. C. 1975. Weathering rinds as a relative-age criterion: Application to subdivision of glacial deposits in the Cascade Range. *Geology* 3:101–104.

Porter, S. C., and G. H. Denton 1967. Chronology of neoglaciation in the North American Cordillera. *American Journal of Science* 265:177–210.

Potter, R. M., and G. R. Rossman 1979. Mineralogy of manganese dendrites and coatings. *American Mineralogist* 64:1219–1226.

Reznichenko, N. V., T. R. Davies, and S. Winkler 2016. Revised palaeoclimatic significance of Mueller Glacier moraines, Southern Alps, New Zealand. *Earth Surface Processes and Landforms* 41:196–207.

Ricker, K. E., T. J. Chinn, and M. J. McSaveney 1993. A late Quaternary moraine sequence dated by rock weathering rinds, Craigieburn Range, New Zealand. *Canadian Journal of Earth Science* 30:1861–1869.

Reed, S. J. B. 2005. *Electron microprobe analysis and scanning electron microscopy in geology*. Cambridge: Cambridge University Press.

Scuderi, L. A. 1987. Late-Holocene upper timberline variation in the southern Sierra Nevada. *Nature* 325:242–244.

Sharp, M., J. Parkes, B. Cragg, I. J. Fairchild, H. Lamb, and M. Tranter 1999. Widespread bacterial populations at glacier beds and their relationship to rock weathering and carbon cycling. *Geology* 27:107–110.

Sharp, M., J. L. Tison, and G. Fierens 1990. Geochemistry of subglacial calcites: implications for the hydrology of the basal water film. *Arctic and Alpine Research* 22:141–152.

Skidmore, M., S. P. Anderson, M. Sharp, J. Foght, and B. D. Lanoil 2005. Comparison of microbial community compositions of two subglacial environments reveals a possible role for microbes in chemical weathering processes. *Applied and Environmental Microbiology* 71:6986–6997.

Souchez, R. A., and M. Lemmens 1985. Subglacial carbonate deposition: an isotopic study of a present-day case. *Palaeogeography, Palaeoclimatology, Palaeoecology* 51:357–364.

Spilde, M. N., P. J. Boston, and D. E. Northup 2007. Growth rate of rock varnish determined from high lead concentrations on rocks at Socorro, New Mexico. *Geological Society of America Abstracts with Programs* 39 (6):105.

Spilde, M. N., L. A. Melim, D. E. Northrup, and P. J. Boston 2013. Anthropogenic lead as a tracer for rock varnish growth: implications for rates of formation. *Geology* 41:263–266.

Thiagarajan, N., and C. A. Lee 2004. Trace-element evidence for the origin of desert varnish by direct aqueous atmospheric deposition. *Earth and Planetary Science Letters* 224:131–141.

Thorn, C. E., R. G. Darmody, J. C. Dixon, and P. Schlyter 2001. The chemical weathering regime of Karkevagge, arctic-alpine Sweden. *Geomorphology* 41:37–52.

Thorn, C. E., J. C. Dixon, R. G. Darmody, and C. E. Allan 2006. Ten years (1994–2004) of "potential" weathering in Kärkevagge, Swedish Lapland. *Catena* 65:272–278.

Tranter, M. 2003. Geochemical weathering in glacial and proglacial environments. In ed. J. I. Drever, *Treatise on geochemistry*. Volume 5., pp. 189–205. Amsterdam: Elsevier.

Vogt, T. 1990. Cryogenic physico-chemical precipitations: Iron, silica, calcium carbonate. *Permafrost and Periglacial Processes* 1:283–293.

Vogt, T., and A. E. Corte 1996. Secondary precipitates in Pleistocene and present cryogenic environments (Mendoza Precordillera, Argentina, Transbaikalia, Siberia, and Seymour Island, Antarctica). *Sedimentology* 43:53–64.

Wadham, J. L., R. De'Ath, F. M. Monteiro, M. Tranter, A. Ridgwell, R. Raiswell, and S. Tulaczyk 2013. The potential role of the Antarctic Ice Sheet in global biogeochemical cycles. E*arth and Environmental Science Transactions of the Royal Society of Edinburgh* 104:55–67.

Wadham, J. L., M. Tranter, M. Skidmore, A. J. Hodson, J. Priscu, W. B. Lyons, and M. Jackson 2010. Biogeochemical weathering under ice: Size matters. *Global Biogeochemical Cycles* 24:DOI: 10.1029/2009GB003688.

Wayne, D. M., T. A. Diaz, R. J. Fairhurst, R. L. Orndorff, and D. V. Pete 2006. Direct major-and trace-element analyses of rock varnish by high resolution laser ablation inductively-coupled plasma mass spectrometry (LA-ICPMS). *Applied Geochemistry* 21:1410–1431.

Whalley, W. B. 1984. High altitude rock weathering processes. In ed. K. J. Miller, *International Karakoram Project Volume One*. Cambridge University Press: Cambridge.

Whalley, W. B., A. F. Gellatly, J. E. Gordon, and J. D. Hansom 1990. Ferromanganese rock varnish in North Norway: a subglacial origin. *Earth Surface Processes and Landforms* 15:265–275.

Whelan, P., and A. J. Bach 2017. Retreating Glaciers, Incipient Soils, Emerging Forests: 100 Years of Landscape Change on Mount Baker, Washington, USA. *Annals of the American Association of Geographers* 107:336–349.

Wilson, P., J. A. Matthews, and R. W. Mourne 2016. Relict Blockstreams at Insteheia, Valldalen-Tafjorden, Southern Norway: Their Nature and Schmidt Hammer Exposure Age. *Permafrost and Periglacial Processes* 28:286–297.

Zasadni, J., and P. Kłapyta 2016. From valley to marginal glaciation in alpine-type relief: Late glacial glacier advances in the Pięć Stawów Polskich/Roztoka Valley, High Tatra Mountains, Poland. *Geomorphology* 253:406–424.